Utah State University

DigitalCommons@USU

All Graduate Theses and Dissertations

Graduate Studies

5-2011

Novel Application of Neutrosophic Logic in Classifiers Evaluated under Region-Based Image Categorization System

Wen Ju
Utah State University

Follow this and additional works at: https://digitalcommons.usu.edu/etd

Part of the Computer Sciences Commons

Recommended Citation

Ju, Wen, "Novel Application of Neutrosophic Logic in Classifiers Evaluated under Region-Based Image Categorization System" (2011). *All Graduate Theses and Dissertations*. 887.
https://digitalcommons.usu.edu/etd/887

UtahStateUniversity
MERRILL-CAZIER LIBRARY

NOVEL APPLICATION OF NEUTROSOPHIC LOGIC IN

CLASSIFIERS EVALUATED UNDER REGION-BASED

IMAGE CATEGORIZATION SYSTEM

by

Wen Ju

A dissertation submitted in partial fulfillment
of the requirements for the degree

of

DOCTOR OF PHILOSOPHY

in

Computer Science

Approved:

_____   _____
Dr. Heng-Da Cheng   Dr. Curtis Dyreson
Major Professor   Committee Member

_____   _____
Dr. Stephen J. Allan   Dr. Vicki H. Allan
Committee Member   Committee Member

_____   _____
Dr. Yangquan Chen   Dr. Byron R. Burnham
Committee Member   Dean of Graduate Studies

UTAH STATE UNIVERSITY
Logan, Utah

2011

ABSTRACT

Novel Application of Neutrosophic Logic in Classifiers Evaluated

under Region-Based Image Categorization System

by

Wen Ju, Doctor of Philosophy

Utah State University, 2011

Major Professor: Dr. Heng-Da Cheng
Department: Computer Science

Neutrosophic logic is a relatively new logic that is a generalization of fuzzy logic. In this dissertation, for the first time, neutrosophic logic is applied to the field of classifiers where a support vector machine (SVM) is adopted as the example to validate the feasibility and effectiveness of neutrosophic logic. The proposed neutrosophic set is integrated into a reformulated SVM, and the performance of the achieved classifier N-SVM is evaluated under an image categorization system. Image categorization is an important yet challenging research topic in computer vision. In this dissertation, images are first segmented by a hierarchical two-stage self-organizing map (HSOM), using color and texture features. A novel approach is proposed to select the training samples of HSOM based on homogeneity properties. A diverse density support vector machine (DD-SVM) framework that extends the multiple-instance learning (MIL) technique is then applied to the image categorization problem by viewing an image as a bag of instances corresponding to the regions obtained from the image segmentation. Using the instance

prototype, every bag is mapped to a point in the new bag space, and the categorization is transformed to a classification problem. Then, the proposed N-SVM based on the neutrosophic set is used as the classifier in the new bag space. N-SVM treats samples differently according to the weighting function, and it helps reduce the effects of outliers. Experimental results on a COREL dataset of 1000 general-purpose images and a Caltech 101 dataset of 9000 images demonstrate the validity and effectiveness of the proposed method.

(69 pages)

To my parents for their endless love and support and to my husband and little son who

made it worth all the sacrifice

ACKNOWLEDGMENTS

First, I would like to express the deepest appreciation to my major professor, Dr. Heng-Da Cheng. His academic guidance, encouragement, and dedication to reviews, analyses, and all other needs have been essential to my research and academic life.

I would also like to thank my other committee members, Dr. Vicki Allan, Dr. Steve Allan, Dr. Curtis Dyreson, and Dr. Yangquan Chen, for guiding and otherwise benefitting my research.

I wish to thank my friends and family for their support and understanding during my study at Utah State University. Especially, my appreciation goes to my parents and my husband, whose support and love for me throughout all my frustration, depression, and hopelessness inspired me to do more with my life.

Wen Ju

CONTENTS

LIST OF TABLES

LIST OF FIGURES

CHAPTER 1

INTRODUCTION

Neutrosophy is a branch of philosophy, which studies the origin and nature of neutralities, as well as their interrelation with different conceptive domains [1]. Neutrosophic logic is a multiple value logic based on neutrosophy. Fuzzy logic extends classical logic by assigning a membership function ranging in degree between 0 and 1 to variables. As a generalization of fuzzy logic, neutrosophic logic introduces a new component called "indeterminacy" and carries more information than fuzzy logic. One could expect that the application of neutrosophic logic would lead to better performance than fuzzy logic. Neutrosophic logic is so new that its use in many fields merits exploration. In this dissertation, for the first time, neutrosophic logic is applied to the field of classifiers. The proposed classifier is then evaluated under an image categorization system to validate its feasibility and effectiveness.

1.1   Neutrosophic Logic

Neutrosophic logic was introduced in 1995 as a generalization of fuzzy logic [1]. At its heart, each proposition is estimated to have a percentage of truth in subset T, a percentage of indeterminacy in subset I, and a percentage of falsity in subset F, where T, I, F are subsets of real numbers from [0, 1]. Here is an example. Jack wants to invite Kate to the homecoming banquet. Kate may or may not accept the invitation. In neutrosophic terms, the statement "Kate will accept the invitation" can be described in the following

way: it is 60% true, 40% indeterminate, and 30% false. Neutrosophic logic is close to human reasoning in the way that it considers the uncertain character of real life.

A neutrosophic set is a generalization of a classical set and a fuzzy set. Generally, a neutrosophic set is denoted as $<T, I, F>$. An element $x(t, i, f)$ belongs to the set in the following way: it is t true, i indeterminate, and f false in the set, where t, i, and f are real numbers taken from sets T, I, and F with no restriction on T, I, F, nor on their sum $m=t+i+f$. Figure 1.1 shows the relationship among classical set, fuzzy set and neutrosophic set. In a classical set, $i = 0$, t and f are either 0 or 1. In a fuzzy set, $i = 0, 0 \leq t, f \leq 1$ and $t + f = 1$. In a neutrosophic set, $0 \leq t, i, f \leq 1$.
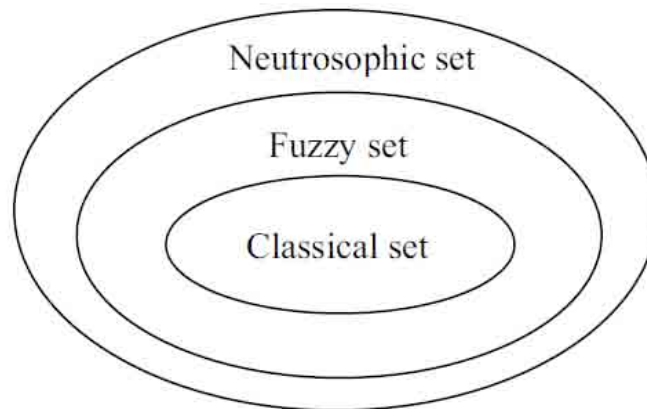
Fig. 1.1: Relationship among classical set, fuzzy set and neutrosophic set.

Neutrosophic logic has been applied to medical and color image processing problems recently. A novel approach for image thresholding is proposed by defining neutrosophic set in image domain in [2]. In [3], neutrosophy is applied to image processing by defining a neutrosophic domain. Image segmentation is then performed in that domain. A region growing algorithm based on neutrosophic logic is implemented for

the automatic segmentation algorithm of breast ultrasound images in [4]. A novel approach for image denoising based on neutrosophic set is proposed in [5]. In this dissertation, for the first time, a neutrosophic set is applied to the field of classifiers where an SVM is adopted as the example to validate the feasibility and effectiveness of neutrosophic logic. This brand new application of neutrosophic logic consists of neutrosophic set that is integrated into a reformulated SVM, and the performance of the achieved classifier N-SVM is evaluated under an image categorization system.

1.2   Image Categorization

With the rapid development of the Internet and digital photography, the size of the average image collection on the web has been growing rapidly in recent years. The semantic meaning associated with an image is usually perceived by human viewers. In order to handle the massive amounts of digital image resources, an automated system that discovers semantic meaning from low-level image features is highly desirable. Image categorization is such a tool that refers to the process of labeling images into one of a set of predefined categories. The computer algorithm learns the relationship between the content of an image and its associated semantic meaning, and then assigns a class label (keyword) to the image accordingly [6].

Image categorization is an important research topic having potential applications in biomedicine, image understanding, digital libraries, remote sensing, web image searching, and surveillance systems, etc. Usually, it is not a very difficult task for humans, but for computers it has proven to be a highly challenging problem because an automatic image categorization system has to distinguish among different categories and

deal with several object types simultaneously in an image [7]. Humans tend to interpret images and measure their similarity using high-level concepts, such as labels (keywords) and text description. However, the features extracted from images by automatic computer vision methods are usually low-level contents, such as color, shape, texture, and spatial layout, etc. In general, there is no direct connection between high-level concepts and low-level content [8]. The discrepancy between the limited descriptive power of low-level image features and the richness of human semantics is usually referred to as the "semantic gap" [9, 10]. Given a set of labeled images, the goal of an image categorization system is to reduce the semantic gap by designing a computer algorithm that automatically learns the semantic concepts from low-level features contained in images. Then, for a previously unseen image, the system will assign a class label to it from a number of predefined categories.

A lot of machine learning techniques have been used widely in the field of image processing [11, 12, 13], and image categorization is of no exception. The techniques used in image categorization could be grouped into two classes: the probabilistic modeling based methods, and the classification based methods.

1.2.1   *Probabilistic Modeling-based Methods*

Probabilistic modeling based methods aim to build a relevance model that represents the connection between images and labels (keywords).

In the work of [14], a set of blob tokens obtained from clustering image regions are translated to a set of keywords through a machine translation model (TM). By assuming that image categorization could be viewed as similar to the cross-lingual retrieval

problem, a cross-media relevance model (CMRM) is proposed in [15]. CMRM is a discrete model that depends on the clustering of feature vectors into blobs, and its performance is highly influenced by the quality of the clustering. The CMRM model is further improved by a continuous space relevance model (CRM) in [16] and a multiple-Bernoulli relevance model (MBRM) in [17]. In CRM, an image is segmented into regions, and each region is represented by a continuous-valued feature vector. Given a set of predefined images, a joint probabilistic model for the link between the image features and their labels is firstly estimated. Then, the probability of image regions belonging to a specific keyword could be predicted using that model. The MBRM is proposed to generate keywords based on the multiple Bernoulli distribution instead of the multinomial one used in CRM. Both CRM and MBRM build the model directly from continuous features without relying on clustering techniques, and consequently they do not have the problem of granularity issues. More recently, a dual cross-media relevance model (DCMRM), which calculates the expectation over keywords in a predefined lexicon, has been proposed to solve the image categorization problem [18].

The probabilistic latent semantic analysis technique (pLSA) is adopted for image classification in [19], which has too many parameters. In order to reduce the number of parameters, the latent Dirichlet allocator (LDA) is incorporated into the pLSA model in [20, 21]. A robust pLSA model using rival penalized competitive learning is introduced in [22] to solve image categorization problem. Carneiro et al. [23] propose a supervised multi-class labeling method, in which a two-level mixture probabilistic model is built to learn the relationship between images and their labels. One of the mixtures is the density

estimated for each image, and the other mixture is associated with all images sharing a common semantic label. The spatial relationship among regions is captured by a Markov random field model, and a maximum a posterior rule is applied to interpret images in [24]. A one-dimensional hidden Markov model (HMM) is proposed for indoor/outdoor scene classification, which is trained over quantized color histograms of image blocks [25]. In the automatic linguistic indexing of pictures (ALIP) system proposed by Li and Wang [26], the keywords are captured by a two-dimensional multi-resolution HMM trained on color and texture features of image blocks. A hierarchical spatial Markov model for image categorization is presented in [27]. Word correlation is also integrated into the categorization process in some studies, such as the coherent language model [28], the wordnet-based method [29], and the correlated label propagation [30].

1.2.2   Classification-based Methods

In contrast to probabilistic modeling-based methods, each semantic label or keyword is regarded as an independent class and corresponds to a classifier in the classification-based methods [31].

Histograms have been used widely in many image categorization problems. The *k*-nearest neighbor classifier is applied to color histograms to discriminate between *indoor* and *outdoor* images in [32]. Support vector machines (SVMs) built on color histogram features are adopted to classify images containing different objects [33]. Vailaya et al. [34] categorize *sunset/forest/mountain* images using Bayesian classifiers over color histograms and categorize *city/landscape* images using the same classifier on edge

directions histograms. Chang et al. apply SVMs and Bayes point machines for image annotation, where color, shape, and wavelet-based texture features are used [35].

The advantage of histograms is their efficient calculation, and the disadvantage of a global histogram representation is that the spatial distribution of images is not considered. Many approaches have been proposed to cope with this drawback. Huang et al. construct a classification tree using color correlograms that extracts the spatial relationship among colors in an image [36]. Gdalyahu and Weinshall adopt local curve matching for shape silhouette classification, where the objects of images are described by their outlines [37]. By dividing an image into blocks, methods based on sub-images have also been proposed to explore the local and spatial properties of images. Gorkani and Picard divide an image into 16 non-overlapping blocks of equal size, and the dominant orientations are calculated for each block [38]. The images are then classified as *city/suburb* scenes, which are determined by the majority of orientations of the blocks. The work in [39] divides an image into a fixed number of partially overlapping subdivisions, and a multi-class SVM is trained to classify an unseen image into one of the predefined categories.

1.3   Proposed Image Categorization System

As discussed in Section 1.2.2, approaches based on sub-images can explore the local and spatial properties of an image. However, a rigid partition of an image into blocks often breaks an object into several blocks. Thus, visual information contained in objects that could be helpful to image categorization may be destroyed in this way. To address this problem, image segmentation could be adopted as a powerful tool to extract object information from an image. Image segmentation is a process of dividing an image into

different regions such that each region is, but the union of any two adjacent regions is not, homogeneous [40]. Image segmentation is a well-studied topic and has been applied to many fields, such as medical image detection and color image classification [3, 41]. In this dissertation, I focus on solving region-based image categorization problem. A hierarchical two-stage self-organizing map (HSOM) is used to decompose an image into a collection of regions. A novel method is proposed to explore the homogeneity property of the image and select training samples for the HSOM.

Recently, multiple-instance learning (MIL) has been applied to image categorization. MIL is a variation of supervised learning, whose task is to learn a concept given positive and negative bags of instances. It assumes that bags and instances share the same set of labels, and a bag receives a positive label if at least one of its instances in the bag is assigned with that label. In the context of the region-based image categorization problem, images are viewed as bags, and regions are viewed as instances.

Diverse density (DD) model is first proposed in [42] to solve the MIL problem. By exploring the distribution of instance feature space, a feature point with a large DD value is selected that is close to all instances in the positive bags and far away from the instances in the negative bags. Upgrading single-instance learning methods, such as decision trees, neural network and SVMs, is a new trend to cope with MIL problems [6, 43, 44, 45, 46]. Two SVM-based formulations of MIL, mi-SVM and MI-SVM, are proposed in [45]. Both algorithms solve the maximum margin problem under MIL constraints by modifying the conventional SVM through an iterative heuristic optimization. Chen and Wang propose a DD-SVM algorithm in [46], which assumes that

the classification of bags is only related to some properties of the bags. Consequently, it solves the MIL problem by transforming the original feature space to a new bag feature space, and training an SVM in the new space. Two sets of SVMs, MIL-based SVMs and global-feature-based SVMs, are integrated to provide the final classification results in [43]. Yang et al. [6] propose an asymmetrical SVM-based MIL algorithm that extends the conventional SVM to the MIL setting by introducing loss functions for false positives and false negatives. Deep SVM is introduced in [47], wherein an SVM is trained in the standard way and the kernel activations of support vectors are used as inputs to train another SVM at the next layer. In this dissertation, the framework of DD-SVM proposed in [46] is adopted in the proposed region-based image categorization system. A novel reformulated SVM based on a neutrosophic set is proposed to replace the standard SVM.

As discussed in Section 1.1, neutrosophic logic is applied to the field of classifiers in this dissertation. I propose a novel neutrosophic set for SVM inputs and combine it with the reformulated SVM which treats samples differently according to the weighting function. The proposed classifier helps reduce the effects of outliers and is applied under a DD-SVM framework to solve the MIL problem in region-based image categorization.

The rest of the dissertation is organized as follows. Chapter 2 presents the image segmentation method based on homogeneity property. Chapter 3 introduces the DD-SVM framework as an extension of the MIL problem. Chapter 4 describes in detail the novel reformulated SVM based on neutrosophic set. The experiment results are presented in Chapter 5, and finally conclusions are drawn in Chapter 6.

CHAPTER 2

IMAGE SEGMENTATION

Image segmentation is the process of dividing an image into non-overlapping regions, such that each region is homogeneous but the joint of any two neighboring regions is non-homogeneous. Segmentation is essential to image processing and pattern recognition. Due to the fact that abundant information is contained in color images and the power of PCs is increasing rapidly, color image segmentation has attracted more and more attention [48].

Neural network approaches have been studied and used a lot in recent years. Self-organizing map (SOM) networks, as a kind of neural network based on the idea of preserving the topology of the original input dataset, were first proposed by Kohonen [49]. Unlike simple competitive learning methods where only the winning neurons are updated to learn, the neurons in the neighborhood of the winning neurons in SOM are also updated in the learning process and lead to an ordered feature-mapping that could be explored in many applications. The limitation of this method is that the final number of classes has to be specified a priori. Lampinen and Oja [50] proposed a hierarchical SOM (HSOM) to solve this drawback. Arbitrarily complex clusters are formed, and the resultant clusters match the desired classes better than the conventional SOM.

In this chapter, an image segmentation method based on color and texture features using a hierarchical two-stage self-organizing map (HSOM) is presented. A novel approach for selecting training samples for the HSOM, based on homogeneity, is proposed. Fig. 2.1 shows the outline of the proposed segmentation method.

```
┌─────────────────┐      ┌─────────────────┐      ┌─────────────────┐
│   Input Image   │─────▶│Feature Extraction│────▶│  Selection of   │
│   (Raw Data)    │      │ (Color & Texture)│      │ Training Samples│
└─────────────────┘      └─────────────────┘      └─────────────────┘

┌─────────────────┐      ┌─────────────────┐      ┌─────────────────┐
│   Two-stage     │─────▶│     Region      │────▶│   Segmented     │
│     HSOM        │      │    Merging      │      │     Image       │
└─────────────────┘      └─────────────────┘      └─────────────────┘
```
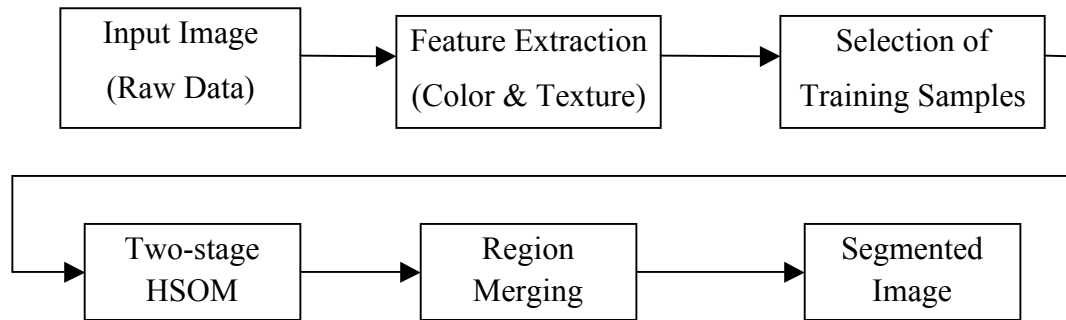
Fig. 2.1: The outline of the proposed image segmentation method.

Section 2.1 describes the feature extraction, and Section 2.2 introduces HSOM. The proposed selection approach for the training samples of HSOM is discussed in detail in Section 2.3. Experimental results are given at the end of this chapter.

2.1 Feature Extraction

In the proposed method, both color and texture features are extracted from the image. Texture refers to a pattern of elements placed closely together in such a manner that the pattern somehow repeats itself. Texture feature contains valuable information and has been used extensively in the research of image processing. Laws [51, 52] developed a coherent set of "texture energy" masks that can be used to extract texture features from images for image segmentation and classification.

The two-dimensional masks used to extract texture features are derived from five simple one-dimensional filters which are:

$$L5 = (\ 1\quad 4\quad 6\quad 4\quad 1\ )$$

$$E5 = (\ -1\quad -2\quad 0\quad 2\quad 1\ )$$

$$S5 = (\,\text{-}1 \quad 0 \quad 2 \quad 0 \quad \text{-}1\,)$$

$$W5 = (\,\text{-}1 \quad 2 \quad 0 \quad \text{-}2 \quad 1\,)$$

$$R5 = (\,1 \quad 4 \quad 6 \quad \text{-}4 \quad 1\,)$$

The letters stand for Level, Edge, Spot, Wave and Ripple. These masks are convolved with the transposes of each other to provide a set of symmetric and anti-symmetric masks, whose center weights are zero-sum except for the Level filters. Four of Laws' most successful masks are shown in Fig. 2.2.

-1	-2	0	2	1
-4	-8	0	8	4
-6	-12	0	12	6
-4	-8	0	8	4
-1	-2	0	2	1

L5E5

-1	0	2	0	-1
-2	0	4	0	-2
0	0	0	0	0
2	0	-4	0	2
1	0	-2	0	1

E5S5

1	-4	6	-4	1
-4	16	-24	16	-4
6	-24	36	-24	6
-4	16	-24	16	-4
1	-4	6	-4	1

R5R5

-1	0	2	0	-1
-4	0	8	0	-4
-6	0	12	0	-6
-4	0	8	0	-4
-1	0	2	0	-1

L5S5

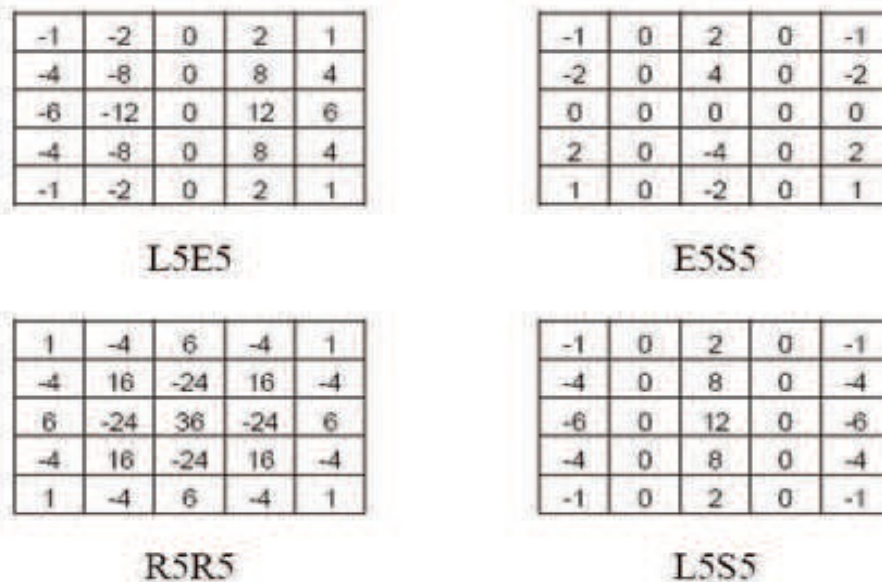Fig. 2.2: Four of Laws' masks for texture feature.

L5E5 is a horizontal edge mask enhancing the horizontal structure in texture. E5S5 is peculiar V-shape mask that responds best to textures with a low correlation. R5R5 is a high-frequency spot detector producing a grainy feature plane that is very difficult to reproduce. L5S5 is a vertical line detector that enhances the vertical edges in the image.

In this work, each pixel in the image is represented by a seven-dimensional vector: {*r, g, b, e5l5, e5s5, r5r5, l5s5*}. The first three components of the feature vector are R, G, and B values for each pixel in the original image. The next four components are obtained by applying the Laws' texture energy measures as introduced above [51].

2.2 Introduction of SOM and HSOM

The basic idea of a self-organizing map (SOM) is simple and effective. An SOM consists of *M* neurons located on a regular low-dimensional grid, usually one- or two-dimensional. The lattice of the grid is either hexagonal or rectangular, as shown in Fig. 2.3.

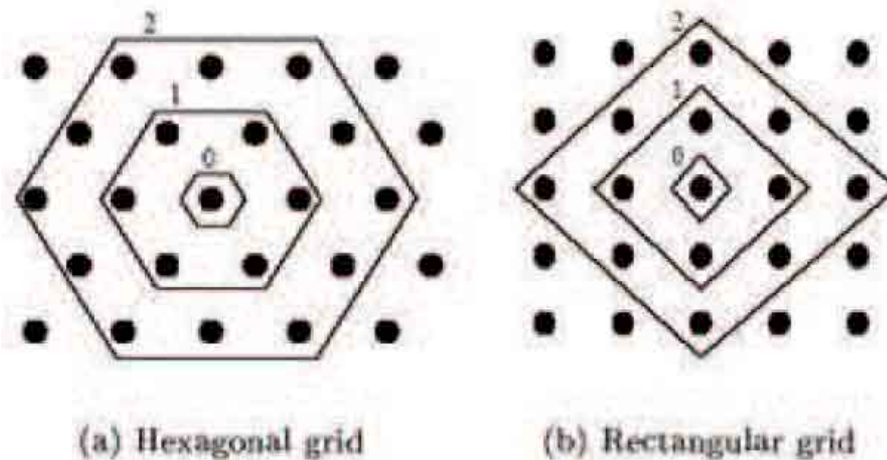(a) Hexagonal grid   (b) Rectangular grid

Fig. 2.3: The SOM neighborhood set for hexagonal and rectangular lattice.

The training mechanism for an SOM is iterative. Each neuron *i* has a *d*-dimensional prototype vector $m_i = [m_{i1}, ..., m_{id}]$. At the beginning of every training step, a sample data vector *x* is randomly chosen from the training set. Distances between *x* and all prototype

vectors are calculated. The best-matching unit (BMU) denoted as b is the map unit with a prototype closest to x:

$$\|x - m_b\| = \min_i \{\|x \quad m_i\|\} \tag{2.1}$$

Next, the prototype vectors are updated. The BMU and its topological neighbors are moved closer to the input vector in input space, as shown in Fig. 2.4. The update rule for the prototype vector of unit i is:

$$m_i(t+1) = m_i(t) + \alpha(t)h_{bi}(t)[x \quad m_i(t)] \tag{2.2}$$

where t denotes time, $\alpha(t)$ is the learning rate, and $h_{bi}(t)$ is a neighborhood kernel centered on the winner unit. An example of a kernel would be the Gaussian kernel:

$$h_{bi}(t) = \exp(-\frac{\|r_b - r_i\|^2}{2\sigma^2(t)}) \tag{2.3}$$

where r_b and r_i are positions of neurons, b and i are on the SOM grid, and $\sigma(t)$ is the neighborhood radius. Both the learning rate $\alpha(t)$ and neighborhood radius $\sigma(t)$ decrease monotonically with time.

During training, the SOM behaves like a flexible net folding onto the "cloud" formed by the training data. Because of the relationships within neighborhood, neighboring prototypes are pulled in the same direction, and prototype vectors of neighboring units resemble each other. Thus, the goal of an SOM is to create a topologically (i.e., locally) ordered mapping of the input samples.
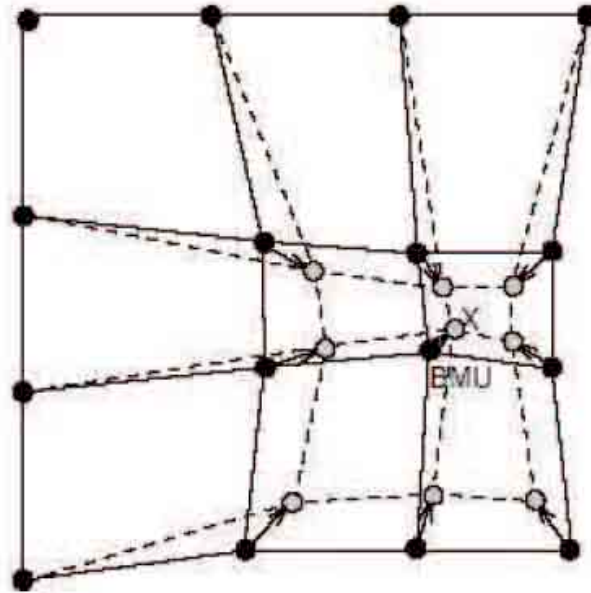
Fig. 2.4: Updating the BMU and its neighbors towards the input sample *x*.
The neuron position before and after the update is represented by the black
and the gray dots, respectively. The lines show neighborhood relations.

The hierarchical SOM (HSOM) can be defined as a two-layer SOM, and its training

mechanism is:

1. For each input vector *x*, the best matching unit is chosen from the first layer map,

and its index *b* is input into the second layer;

2. The best matching unit for input *b* is chosen from the second layer map, and its

index is the output of the network.

In a conventional self-organizing map (SOM) network, the number of regions in the

final segmented image relies on the number of neural units in the Kohonen layer. But it is

highly improbable that the number of regions in an image is known a priori. This

significant shortcoming is overcome by implementing a hierarchical SOM as a pattern

classifier to group the output neurons into subsets, each of which corresponds to a discrete region. The HSOM used in this dissertation has 100 output neurons arranged in a 10 x 10 grid in the first stage and 20 neurons in the second stage.

2.3   Selection of Training Samples
        Based on Homogeneity

Literature that discusses the selection of the samples for training the SOM is scarce. Random selection is most commonly used to select the training samples for an HSOM. While random selection ensures an unbiased collection of training samples, it does not always provide the optimal set of training samples. In the case of image segmentation, the pixels around the boundary of the perceptual segments provide more information and should be emphasized in the training procedure. Therefore, a novel approach for selecting training samples is proposed in this dissertation.

The selection criterion is based on a definition of homogeneity β_{ij} for pixel (i, j) in a gray image proposed in [52], which is composed of the following five components:

1. Edge value:
$$e_{ij} = \sqrt{s_1^2 + s_2^2} \tag{2.4}$$

where s_1 and s_2 are the results of applying the row and column masks of the Sobel edge detector, respectively.

2. Standard deviation:
$$v_{ij} = \sqrt{\frac{1}{d^2} \sum_{p=i-\frac{d-1}{2}}^{i+\frac{d-1}{2}} \sum_{q=j-\frac{d-1}{2}}^{j+\frac{d-1}{2}} (g_{pq} - \mu_{ij})^2} \tag{2.5}$$

where u_{ij} is the mean of the gray levels within the window w_{ij} centered at (i, j) of size d.

3. Entropy:
$$h_{ij} = -\frac{1}{2\log d}\sum_{k=1}^{L} P_k \log P_k \qquad (2.6)$$

where P_k is the probability of the kth gray level, which can be calculated as $\dfrac{n_k}{d^2}$, n_k is the

total number of pixels with the kth gray level, and L is the total number of gray levels in

the window w_{ij}.

4. Skewness:
$$\gamma_{3ij} = \frac{\displaystyle\sum_{p=i-\frac{d-1}{2}}^{i+\frac{d-1}{2}}\sum_{q=j-\frac{d-1}{2}}^{j+\frac{d-1}{2}}(g_{pq}-\mu_{ij})^3}{(N-1)\sigma_{ij}^3} \qquad (2.7)$$

5. Kurtosis:
$$\gamma_{4ij} = \frac{\displaystyle\sum_{p=i-\frac{d-1}{2}}^{i+\frac{d-1}{2}}\sum_{q=j-\frac{d-1}{2}}^{j+\frac{d-1}{2}}(g_{pq}-\mu_{ij})^4}{(N-1)\sigma_{ij}^3} - 3 \qquad (2.8)$$

where σ is the standard deviation over N observations.

The homogeneity measure β_{ij} is the normalized value of A_{ij} which is defined as:

$$A_{ij} = (1-E_{ij})\times(1-V_{ij})\times(1-H_{ij})\times(1-R_{3ij})\times(1-R_{4ij}) \qquad (2.9)$$

where E, V, H, R_3 and R_4 are the normalized value of those defined in Eq. (2.4) to Eq.

(2.8), respectively. The more uniform the local region surrounding a pixel is, the larger

the homogeneity value β_{ij} for that pixel.

The homogeneity measure β_{ij} defined above holds only for grayscale images. In

order to be used in a color image, the concept is extended to the domain of RGB images.

Suppose β_{Rij}, β_{Gij}, and β_{Bij} are the homogeneity measures calculated in the R, G, and B

color planes, respectively, the homogeneity measure for the pixel *(i, j)* in the RGB domain can be defined as:

$$\beta_{RGB_{ij}} = 0.33 \times \beta_{R_{ij}} + 0.33 \times \beta_{G_{ij}} + 0.33 \times \beta_{B_{ij}} \tag{2.10}$$

The non-homogeneity measure in the RGB domain can be calculated as:

$$\varphi_{RGB_{ij}} = 1 - \beta_{RGB_{ij}} \tag{2.11}$$

The steps of the proposed algorithm are:

1. A location set Φ is defined to contain the pixel locations of all training samples and is initialized to empty.

2. The average non-homogeneity value is calculated for the entire image as:

$$\mu_{\varphi_{image}} = \frac{1}{MN} \sum_{p=0}^{M-1} \sum_{q=0}^{N-1} \varphi_{RGB_{pq}} \tag{2.12}$$

3. The image is divided into blocks of arbitrary size *d*d* (in this dissertation, *d=15*), and the local average nonhomogeneity value for each block *t* is calculated as:

$$\mu_{\varphi_{block}} = \frac{1}{d^2} \sum_{p=i-\frac{d-1}{2}}^{i+\frac{d-1}{2}} \sum_{q=j-\frac{d-1}{2}}^{j+\frac{d-1}{2}} \varphi_{RGB_{pq}} \tag{2.13}$$

4. For each *d*d* block *t* of the image, the number of pixels to be chosen for training is decided by the threshold:

$$n_{training} = \begin{cases} \max\{10, \ (\mu_{\varphi_{block}} - \mu_{\varphi_{image}}) * d^2\} & if\,(\mu_{\varphi_{block}} - \mu_{\varphi_{image}} \quad 0) \\ 10 & if\,(\mu_{\varphi_{block}} - \mu_{\varphi_{image}} <= 0) \end{cases} \tag{2.14}$$

5. $n_{training}$ pixel locations are then randomly selected from that block t and are added to the location set Φ.

6. Repeat steps 2-4 for all the blocks in the image.

7. The vectors corresponding to the locations in set Φ are then extracted from the HSOM input matrix to form the final training set.

The algorithm ensures that the training dataset contains more pixels representing the diverse regions in the image than those representing the homogeneous regions. Therefore, a training dataset generated in this way carries more information about the image than the training dataset obtained by random selection, and it leads to better results of segmentation.

The output of the HSOM is often an over-segmented image. Hence, the region-merging process in [53, 54] is carried out to combine regions that are similar to each other. After this step, the final segmented image is generated.

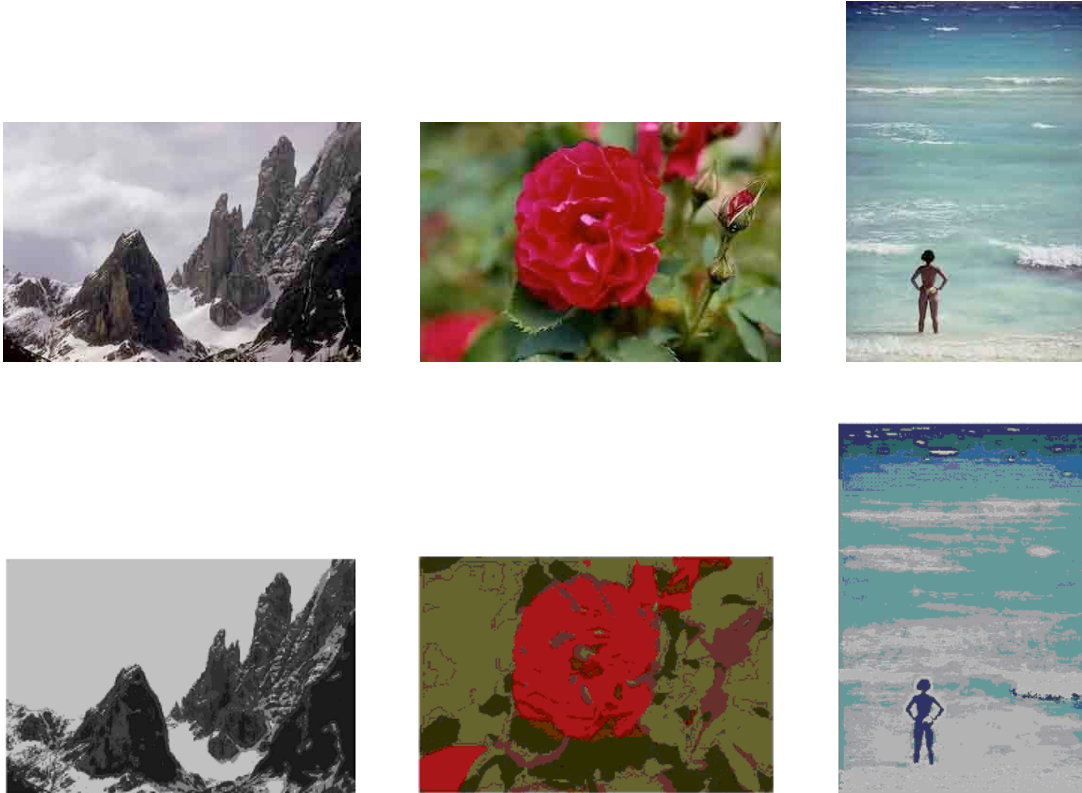Examples of the segmentation results are shown in Fig. 2.5.

Fig. 2.5: Segmentation results by HSOM based on homogeneity measure.
First row: Original images; Second row: Segmented images, respectively.

CHAPTER 3

DIVERSE DENSITY-SUPPORT VECTOR

MACHINE FRAMEWORK

Multiple-instance learning (MIL) is a variation of supervised learning, whose task is to learn a concept given positive and negative bags of instances. The standard MIL problem assumes that bags and instances share the same set of labels. A bag is labeled positive if at least one of its instances is positive, and the bag is labeled negative if all of its instances are negative. To view the image categorization problem in MIL terms, an image is considered as a bag that contains a number of instances corresponding to the regions obtained from the image segmentation. Different bags may have different numbers of instances. For a particular category, a positive label means that the image belongs to it, and a negative label means that the image does not belongs to it.

Chen and Wang proposed a diverse density-support vector machine (DD-SVM) algorithm that extends the standard MIL and applied it to the problem of region-based image categorization [46]. DD-SVM assumes that a positive bag must contain some number of instances satisfying various properties, which are captured by bag features. Each bag feature is defined by an instance in the bag and an instance prototype derived from the DD function. Therefore, the bag features summarize the bag from several aspects. The basic idea of the DD-SVM framework is to map every bag to a point in a new feature space, named the bag feature space, and to train SVMs in the bag feature space.

Now let us describe the DD-SVM in mathematical representation. After the segmentation process in Chapter 1, the mean of the set of feature vectors belonging to each region is calculated and denoted as the region feature vector *x*, which is also called the instance feature vector in terms of the MIL problem. An image B_i, which is segmented into N_i regions $\{R_j : j = 1,...,N_i\}$, is represented by a collection of region feature vectors $\{x_{ij} : j = 1,...,N_i\}$. Let *D* be the labeled dataset, which consists of *l* bag/label pairs, i.e., $D = \{(B_1, y_1),...,(B_l, y_l)\}$, where $y_i \in \{1,-1\}$. The diversity density (DD) function over the instance feature space is defined as:

$$DD_D(x,w) = \prod_{i=1}^{l} [\frac{1+y_i}{2} - y_i \prod_{j=1}^{N_i} (1 - e^{-\|x_{ij}-x\|_w^2})] \tag{3.1}$$

Here, *x* is a point in the instance feature space, *w* is a weight vector defining which features are considered important and which are considered unimportant [38]. $\|.\|_w$ denotes a weighted norm defined by:

$$\|x\|_w = [x^T Diag(w)^2 x]^{\frac{1}{2}} \tag{3.2}$$

where Diag(*w*) is a diagonal matrix whose (*i*, *i*)-th entry is the *i*-th component of *w*.

The values of the DD function are always between 0 and 1. If *x* is close to instances from different positive bags, and at the same time, far away from instances in all negative bags, the value of the DD function is close to 1. Thus, it measures a co-occurrence of instances from different positive bags.

The DD function defined in Eq. (3.1) is a continuous and highly nonlinear function with multiple local maximums and minimums. A larger value of the DD function at a

point indicates a higher probability that the point fits better with the instances from positive bags than with those from negative bags. Thus, the local maximums of the DD function could be selected as instance prototypes that represent a class of instances that is more likely to appear in positive bags than in negative bags. Learning instance prototypes then becomes an optimization problem, which is finding local maximums of the DD function in a high-dimensional space. Gradient-based methods are applied to solve this optimization problem.

Each instance prototype represents a class of instances that is more likely to appear in the bags with the specific label than in the other bags. A bag feature space is then constructed using the instance prototypes, each of which defines one dimension of the bag feature space. Let $\{(x_k^*, w_k^*) : k = 1,...,n\}$ be the collection of instance prototypes, the bag feature $\phi(B_i)$ is defined as:

$$\phi(B_i) = \begin{bmatrix} \min_{j=1,...,N_i} \left\| x_{ij} - x_1^* \right\|_{w_1^*} \\ \min_{j=1,...,N_i} \left\| x_{ij} - x_2^* \right\|_{w_2^*} \\ M \\ \min_{j=1,...,N_i} \left\| x_{ij} - x_n^* \right\|_{w_n^*} \end{bmatrix} \tag{3.3}$$

Using the definition in Eq. (3.3), every bag is mapped to a point in the bag feature space [46]. The region-based image categorization problem is now transformed into a classification problem. SVMs are trained in the bag feature space to serve as classifiers.

CHAPTER 4

NOVEL REFORMULATED SUPPORT VECTOR MACHINE

BASED ON NEUTROSOPHIC SET

In this dissertation, I use the same DD-SVM framework as presented in Chapter 3, except that instead of using standard SVMs in the bag feature space, a novel reformulated SVM based on a neutrosophic set is proposed and applied.

4.1 Background of SVM

Introduced by Vapnik [55], support vector machines (SVMs) are based on statistical learning theory. They have been studied in the framework of structural risk minimization (SRM), which is an inductive principle for learning from a finite training dataset and are useful in working with small-sized samples.

Given a training set S containing n labeled points $(x_1, y_1),\dots, (x_n, y_n)$, where $x_j \in R^N$ and $y_j \in \{-1, 1\}, j=1, \dots, n$. Suppose the positive and negative samples can be separated by some hyperplane. This means there is a linear function between the positive and negative samples with the form:

$$d(x) = w \cdot x + b \qquad (4.1)$$

For each training sample x_j, $d(x_j) \geq 1$ if $y_j = 1$; $d(x_j) < -1$, otherwise. This function is also called as decision function. A test sample x can be classified as:

$$y = sign\big(d(x)\big) \qquad (4.2)$$

For a given training dataset, many possible hyperplanes could be found to separate the two classes correctly. SVM aims to find an optimal solution by maximizing the margin around the separating hyperplane. The solution for a case in two-dimensional space has an optimal separating line, as shown in Figure 4.1.
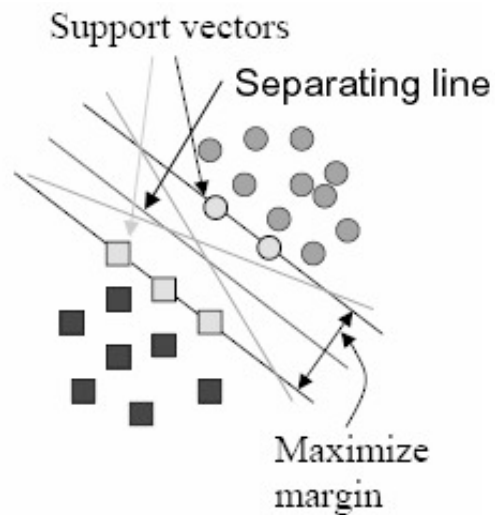
Figure 4.1: An optimal separating line for a two-dimensional space case.

The support vectors are the points on the hyperplanes:

$$y_j\left(w \cdot x_j + b\right) = 1 \qquad (4.3)$$

For another sample $\{x_i, y_i\}$ that is not on the support vector hyperplanes, it has:

$$y_j\left(w \cdot x_j + b\right) > 1. \qquad (4.4)$$

Mathematically, the margin M between two support vectors is finally obtained by:

$$M = \frac{2}{\|w\|} \qquad (4.5)$$

where $\|w\|$ is the norm of w.

Thus, maximizing the margin M is equivalent to minimizing $\|w\|$ with the constraint that there is no sample between the support vector hyperplanes. This constraint can be described as:

$$y_j\left(w\cdot x_j + b\right) \geq 1 \qquad (4.6)$$

In the case that the original samples could not be separated by any hyperplane, SVM will transform the original samples into a higher dimensional space by using a nonlinear mapping. Here, $\varPhi(x)$ denotes the mapping from R^N to a higher dimensional space Z. A hyperplane needs to be found in the higher dimensional space with maximum margin as:

$$w\cdot z + b = 0 \qquad (4.7)$$

such that for each point (z_j, y_j), where $z_j = \varPhi(x_j)$:

$$y_j(w\cdot z_j + b) \geq 1, \quad j = 1, \mathrm{K}, n. \qquad (4.8)$$

When the dataset is not linearly separable, the soft margin is allowed by introduction of n non-negative variables, denoted by $\xi = (\xi_1, \xi_2, \ldots \xi_n)$, such that the constraint for each sample in Eq. (4.8) is rewritten as:

$$y_j(w\cdot z_j + b) \geq 1 - \xi_j, \quad j = 1, \mathrm{K}, n. \qquad (4.9)$$

The optimal hyperplane problem is the solution to the problem:

$$\text{minimize} \frac{1}{2} w\cdot w + C\sum_{j=1}^{k} \xi_j \qquad (4.10)$$

$$\text{subject to} \quad y_j(w \cdot z_j + b) \ge 1 - \xi_j, \, j = \ 1, \text{K}, n. \tag{4.11}$$

where the first term in Eq. (4.10) measures the margin between support vectors, and the second term measures the amount of misclassifications. *C* is a constant parameter that tunes the balance between the maximum margin and the minimum classification error. Then, for a test point $\hat{x}$ which is mapped to $\hat{z}$ in the feature space, the classification result $\hat{y}$ is given as:

$$\hat{y} = sign(w \cdot \hat{z} \quad b) \tag{4.12}$$

4.2 Fuzzy SVM

Lin and Wang propose fuzzy support vector machine in [56]. A membership s_j is assigned for each input sample *(x_j, y_j)*, where $0 < s_j < 1$. Since the membership s_j is the attitude of the corresponding point x_j toward one class, and the parameter ξ_j is a measure of error in the SVM, the term $s_j \xi_j$ is a measure of error with different weighting. The optimal hyperplane problem is then regarded as the solution to:

$$\text{minimize} \ \frac{1}{2} w \cdot w + C \sum_{i=1}^{k} s_j \xi_j \tag{4.13}$$

$$\text{subject to} \ y_j(w \cdot z_j + b) \ge 1 - \xi_j, \, j = \ 1, \text{K}, n. \tag{4.14}$$

In order to use FSVM, a membership function needs to be defined for each input sample. Here, I use the membership function definition proposed in [57]. From Eq. (4.10) one can see that if the ξ_i of a misclassified data x_i is increased, the newly learned hyperplane will have a tendency to correctly classify x_i in order to eliminate the larger
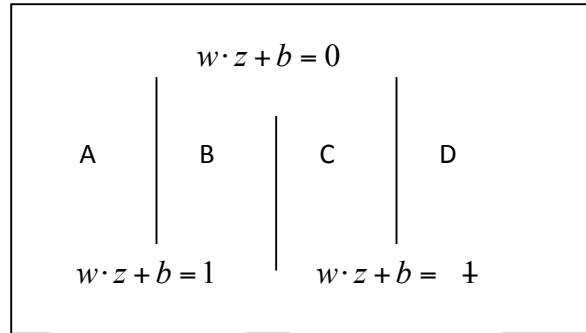
Fig. 4.2: Different regions in high dimension space.

error that x_i introduced to the classifier and finally minimize Eq. (4.10). Correspondingly in Eq. (4.13), assigning a larger membership s_i for an input increases the probability of correctly classifying that sample while a smaller membership decreases the probability of correctly classifying the sample. Based on this observation, the membership function is defined as follows.

1. First, a traditional SVM is trained using the original training set.

2. After step 1, the hyperplane $w \cdot z + b = 0$ is found. Assuming that if $w \cdot z + b > 0$, the data is assigned to the positive class; otherwise, the data is assigned to the negative class. There also are two other hyperplanes $w \cdot z + b = 1$ and $w \cdot z + b = -1$. As indicated in Fig. 4.2, the high dimension space is divided into four regions by these three hyperplanes. For the positive samples, region A represents the input points that are correctly classified and the associated ξs are 0. Region B represents the input points that are also correctly classified but the associated ξs are non-zero. Region C and D represents the input points that are incorrectly classified. For the negative samples, similar regions with the same properties as for the positive samples can be obtained by simply swapping the region positions. In the following discussion, only consider

positive cases are considered. Applying these same principles to negative cases is straightforward.

3. The points in region A have no contribution to the optimization Eq. (4.13) since their ξs are 0. Thus, no matter what membership is assigned to them, it will not affect the resultant hyperplane. Here for simplicity, a constant value $s_A = s_1$ is assigned to them where $0 < s_1 < 1$.

4. The points in region B are correctly classified, but they have non-zero ξs. Thus, they contribute to the optimization equation but should be treated as less important than the points in regions C and D, since they are correctly classified. The more near to the hyperplane $w \cdot z + b > 0$, the more important in the next training procedure to achieve a better classification result. Given $d = w \cdot z + b$, where $z = \Phi(x)$ for input point x, the membership for region B is defined as:

$$s_B = s_1 + (1 - d) \times s_2 \tag{4.15}$$

where $s_2 > 0$, $0 < s_1 + s_2 < 1$ and $0 \le d \le 1$ in region B.

5. The points in region C are incorrectly classified. It can be predicted that in the next training procedure, the hyperplane can move towards these points, thus allowing more of them can be classified correctly. The nearer the points to the hyperplane $w \cdot z + b > 0$, the less important they are in the next training procedure. As explained in step 4, however, they are more important than the points in region B. Using the same notation as step 4, the fuzzy membership for region C is defined as:

$$s_C = (s_1 + s_2) + |d| \times s_3 \tag{4.16}$$

where $s_3 > 0$, $0 < s_1 + s_2 + s_3 < 1$, and $-1 \le d \le 0$ in region C.

6. The points in region D are incorrectly classified. The further away the points are from the hyperplane $w \cdot z + b > 0$, the more probably an outlier exists; thus, the smaller membership should be assigned. The membership for region D is defined as:

$$s_D = (s_1 + s_2 + s_3)/|d|^k \qquad (4.17)$$

where k>0 and $d \leq -1$ in region D. Here, k is a positive integer, and the larger k is, the faster the membership decreases with the increase of distance d. The value of k is chosen as 9 in the experiment.

7. With the memberships defined in steps 3-6, an FSVM is trained and the obtained FSVM is used as a classification tool.

Above, are the steps to design the proposed membership function. The defined membership function is shown in Fig. 4.3.

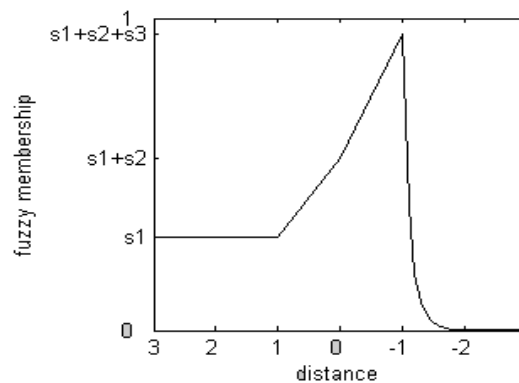Fig. 4.3: Defined membership function.

The parameters s_1, s_2, s_3 are adjustable. They are initialized under the constraint that all of them are positive and the sum of them is smaller than 1. An FSVM is trained using the resultant membership function from those initial parameters. Then, the same training data is used as the test data on the trained FSVM and those three parameters are adjusted

to achieve the highest classification results. Finally, the trained FSVM is used to classify the actual test data.

4.3 Reformulated SVM

A similar idea as the fuzzy SVM introduced in Section 4.2 is adopted in the reformulated SVM. The difference is that the membership s_j is substituted by weighting function g_j where $g_j > 0$. Different inputs contribute differently to the training procedure, and the weighting function g_j is used to evaluate the degree of importance for each input. The value of g_j is a positive number, and it does not necessarily need to be smaller than 1. Now, the optimal hyperplane problem in the reformulated SVM is the solution to:

$$\text{minimize } \frac{1}{2} w \cdot w + C \sum_{j=1}^{k} g_j \xi_j \qquad (4.18)$$

$$\text{subject to } y_j (w \cdot z_j + b) \geq 1 - \xi_j, \ j = 1, \text{K}, n. \qquad (4.19)$$

4.4 Neutrosophic Set

The neutrosophic set is a generalization of the classical set and fuzzy set [1]. In classical theory, there are only <A> and <Non-A>. The degree of neutralities <Neut-A> is introduced and added in neutrosophic theory. Generally, a neutrosophic set is denoted as <T, I, F>. An element $x(t, i, f)$ belongs to the set in the following way: it is t true in the set, i indeterminate in the set, and f false, where t, i, and f are real numbers taken from the sets T, I, and F with no restriction on T, I, F, nor on their sum $m=t+i+f$. The major difference between a neutrosophic set (NS) and a fuzzy set (FS) is that there is no limit on the sum m in a neutrosophic set, while in a fuzzy set m ($m=t+f$) must be equal to 1.

Many research results have shown that the standard SVM is very sensitive to outliers. Here, I propose a neutrosophic set for the input samples of SVM based on the distances between the sample and the class centers. The neutrosophic set explores the spatial distribution of the training samples and can help solve the problems of outliers when integrated into the reformulated SVM.

Using the same notations as in Section 4.1, the neutrosophic set for input samples are denoted as a sequence of points $(x_j, y_j, t_j, i_j, f_j)$, $j = 1, ..., n.$. For the statement that "an example x_j belongs to class y_j", it is t_j true, i_j indeterminate, and f_j false. The center of positive samples C_+, the center of negative samples C_-, and the center of all samples C_{all} are defined as the following:

$$C_+ = \frac{1}{n_+} \sum_{k=1}^{n_+} x_k, \quad C_- = \frac{1}{n_-} \sum_{k=1}^{n_-} x_k,$$

$$C_{all} = \frac{1}{n} \sum_{k=1}^{n} x_k$$

(4.20)

where n_+ is the number of positive samples and n_- is the number of negative samples.

I denote U as the whole input samples set, P as the positive samples subset, and N as the negative samples subset. For positive samples where $y_j = 1$, the neutrosophic components are defined as:

$$t_j = 1 - \frac{\|x_j - C_+\|}{\max_{x_k \in P} \|x_k - C_+\|}$$

$$i_j = 1 - \frac{\|x_j - C_{all}\|}{\max_{x_k \in U} \|x_k - C_{all}\|}$$

(4.21)

$$f_j = 1 - \frac{\|x_j - C_-\|}{\max_{x_k \in P} \|x_k - C_-\|}$$

where $\|x\|$ denotes the Euclidean distance of variable x. For negative samples where $y_j = -1$, the neutrosophic components are defined as:

$$t_j = 1 - \frac{\left\|x_j - C_-\right\|}{\max_{x_k \in N}\left\|x_k - C_-\right\|}$$

$$i_j = 1 - \frac{\left\|x_j - C_{all}\right\|}{\max_{x_k \in U}\left\|x_k - C_{all}\right\|} \qquad (4.22)$$

$$f_j = 1 - \frac{\left\|x_j - C_+\right\|}{\max_{x_k \in N}\left\|x_k - C_+\right\|}$$

With the above definition, every input sample is associated with a triple $<t_j, i_j, f_j>$ as its neutrosophic components. The larger t_j it has, the higher the probability it belongs to the labeled class. The larger i_j it has, the higher the probability it is indeterminate. The larger f_j it has, the higher the probability it belongs to the opposite of the labeled class. The triple contains valuable information extracted from the spatial distribution of the training samples and provides helpful clues in the classifier design.

For the image categorization problem considered in this dissertation, there are usually more than two categories in the dataset. Since SVM is a binary classifier that can only classify the inputs as positive or negative, an appropriate multi-class approach is needed to handle several categories here. Two common methods are "one-against-one" and "one-against-the-rest." For one-against-one, an SVM is trained for each pair of two classes, that is, $\frac{m \times (m-1)}{2}$ SVMs are generated for m categories to accomplish the task. For one-against-the-rest, an SVM is trained to classify one category against all the others together, that is, m SVMs are generated for m categories. Clearly one-against-one is more

time-consuming; thus the one-against-the-rest strategy is applied more widely in categorization problems.

Using the one-against-the-rest strategy, one category is selected as the positive class, and all the other categories together are regarded as the negative class. Usually, the number of images in each category is roughly the same. Thus, the number of samples in the negative class is *m-1* times of the number of samples in the positive class for *m* categories. This makes an unbalanced dataset for the SVM to train. If I still use the definitions in Eq. (4.20), the center of all samples C_{all} is very near to the center of negative samples C_{-} due to the unbalance property of the dataset. But what I really expect is that C_{all} represents the center of the samples in view of data distribution. That is, the distance between C_{all} and the positive group is roughly the same as the distance between C_{all} and the negative group. For examples, if I am given a dataset consisting of four one-dimensional points with coordinates as 3, 25, 30, and 35, point 3 is the positive sample, while the points 25, 30, and 35 are the negative samples. From the data distribution, I expect that the center of all points C_{all} is around the point with coordinate 16.5. However, the center C_{all} calculated using Eq. (4.20) is 23.25, which is more adjacent to the negative samples. To solve this problem, one can view point 3 as appearing three times. In other words, there are three points in the positive class, which are all the same as coordinate 3. Using the same Eq. (4.20) but using the dataset consisting of 6 points (3, 3, 3, 25, 30, 35), the center C_{all} is calculated as 16.5 which is what I expect. In this way, the unbalance property is reduced between the positive and negative samples, without introducing any new samples other than old ones to the training dataset. In terms of mathematics

representation, C_{all} calculated using the above method is actually the mean of the center

of negative samples C_-, and the center of positive samples C_+. So generally speaking, to

eliminate the effect of an unbalanced dataset, a simple but effective modification could be

made to Eq. (4.20) as:

$$C_+ = \frac{1}{n_+} \sum_{k=1}^{n_+} x_k, \, C_- = \frac{1}{n_-} \sum_{k=1}^{n_-} x_k,$$

$$C_{all} = \frac{1}{2}(C_+ + C_-)$$

(4.23)

If the dataset is balanced such that the number of positive samples is roughly the

same as the number of negative samples, C_{all} defined in Eq. (4.23) is almost the same as

the result calculated using Eq. (4.20). For an unbalanced dataset, the modified formula

eliminates the effect of unbalance, and the resulting C_{all} represents the center of all the

samples in the view of data distribution.

4.5 Integrating Neutrosophic Set
with Reformulated SVM

In order to use the reformulated SVM, a weighting function for input samples should

be defined. Following the steps in Section 4.4, every sample has been associated with a

triple $<t_j, i_j, f_j>$ as its neutrosophic components. A larger t_j means the sample is nearer to

the center of the labeled class and is less likely an outlier. So, t_j should be emphasized in

the weighting function. A larger i_j means the sample is harder to be discriminated

between two classes. This factor should also be emphasized in the weighting function in

order to classify the indeterminate samples more accurately. A larger f_j means the sample

is more likely an outlier. This sample should be treated less importantly in the training procedure. Based on these analyses, the weighting function g_j is defined as:

$$g_j = t_j + i_j - f_j \qquad\qquad (4.24)$$

After integrating the proposed weighting function into the reformulated SVM introduced in Section 4.3, training samples are utilized differently in the training procedure according to their spatial distribution. Thus, the proposed classifier, denoted as neutrosophic-support vector machine (N-SVM), reduces the effects of outliers in the training samples and improves the performance when compared to a standard SVM.

CHAPTER 5

EXPERIMENTAL RESULTS AND DISCUSSION

The proposed region-based image categorization method was evaluated on two datasets: COREL 1000 dataset and Caltech 101 dataset. Section 5.1 describes the image datasets and training strategy for classifiers. The performances among the proposed N-SVM, the traditional SVM, and fuzzy SVM are compared and analyzed in Section 5.2. Section 5.3 evaluates the effective of the proposed segmentation method. The effects of an unbalanced dataset are examined in Section 5.4.

5.1 Image Dataset and Training Strategy

The COREL dataset used in this dissertation consists of 1000 general-purpose images [58]. All the images are in JPEG format with a size of either 256×384 or 384×256. There are ten diverse image categories in the dataset, each containing 100 images. The categories are: African people and villages, beach, historical buildings, buses, dinosaurs, elephants, flowers, horses, mountains and glaciers, and food. Some randomly selected sample images from each category are shown in Fig. 5.1.

Caltech 101 dataset is also used here. It contains a total of 9146 images, split between 101 distinct objects (including faces, watches, ants, pianos, etc.) and a background category (make a total of 102 categories). The background category is not used in this dissertation. The number of images per category varies from 31 to 800. In order to make a robust comparison, I have discarded 15 categories that contain less than 40 samples.
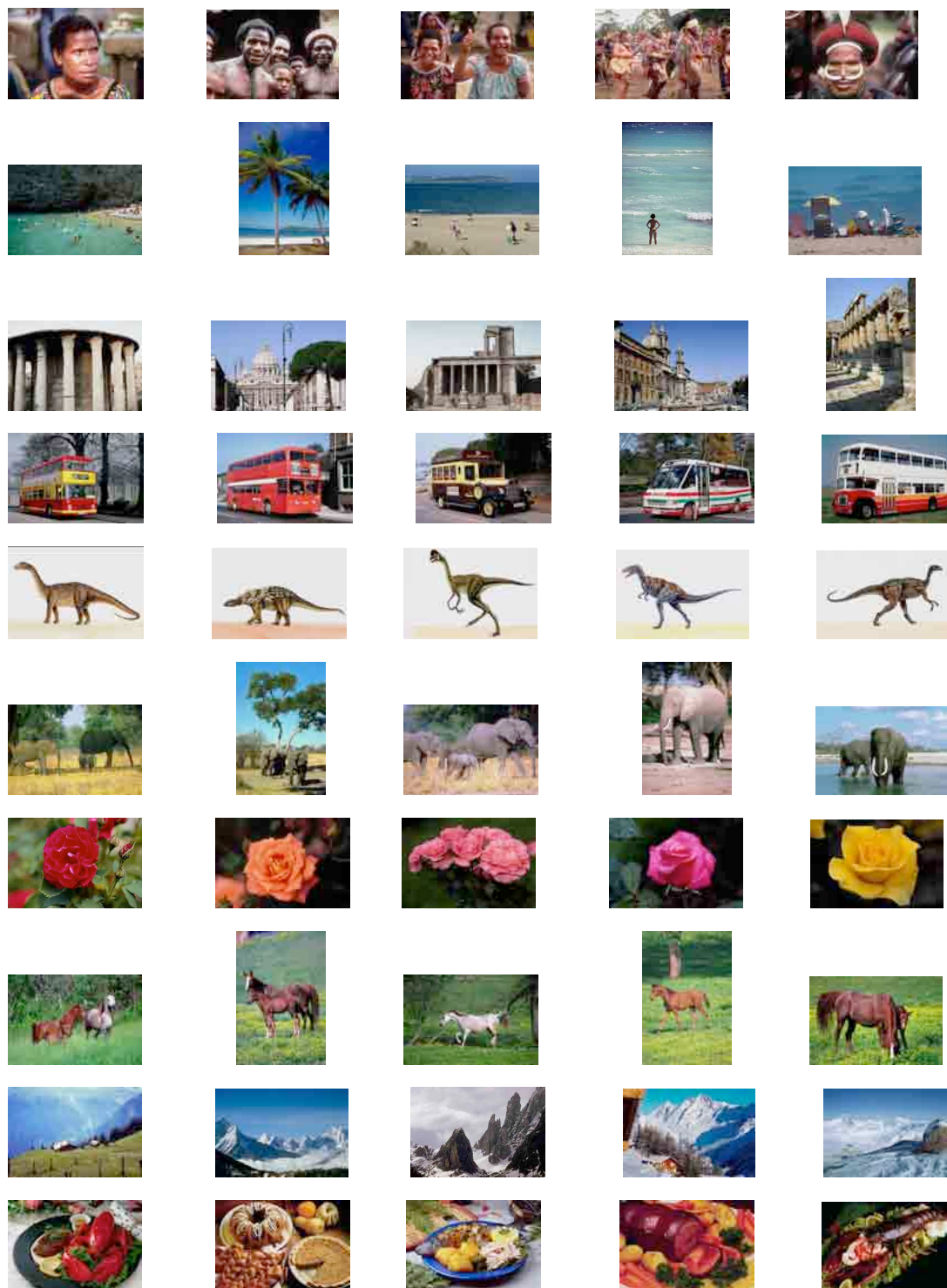
Fig. 5.1: Sample images from COREL dataset.

To evaluate the performance of the proposed N-SVM, a traditional SVM and a fuzzy SVM were also trained and applied to the region-based image categorization problem for comparison. The differences among these classifiers are the restriction for finding the optimal hyperplane. In a fuzzy SVM, membership function s_j is introduced and multiplied to the error parameter ξ_j in Eq. (4.13) as compared to the traditional SVM in Eq. (4.10). Membership function s_j is substituted by weighting function g_j in N-SVM, as shown in Eq. (4.18). After the optimal hyperplane is solved, the same classification criterion is applied to all classifiers, as shown in Eq. (4.12). In our experiments, all the classifiers (SVM, fuzzy SVM, and N-SVM) are trained using the same strategy. The one-against-the-rest method is used to solve the multi-class problem: (a) for each category, a classifier is trained to separate that category from all other categories; (b) the final predicted class label is decided by the winner of all classifiers, that is, the one with the maximum value inside the $sign(\cdot)$ function in Eq. (4.12). For the COREL dataset, images within each category are randomly divided into a training set (50 images) and a test set (50 images). For each category in the Caltech 101 dataset, 30 images are randomly selected as a training set and 50 (or less if they are the remainder) different images are randomly selected as test set. For each SVM designed for category i as positive samples, the training sets of all the categories other than category i are put together as the negative samples. Each experiment is repeated for five random splits, and the average of the classification results obtained over five different test sets is reported.

5.2 Comparison of the Proposed N-SVM with
Traditional SVM and Fuzzy SVM

The proposed N-SVM is a reformulated SVM designed to reduce the effects of outliers in the training samples. To validate its performance, the classification results of the categorization problem were compared to the results obtained from the traditional SVM. Recently, a fuzzy SVM has been applied to many fields including bioinformatics, image retrieval, and text categorization [57, 59, 60]. Since neutrosophic logic is a generalization of fuzzy logic, it is very meaningful to compare the performance between the fuzzy SVM and the proposed N-SVM. So, in this section the comparison focuses on the classification performance among the proposed N-SVM, the traditional SVM, and the fuzzy SVM as introduced in Section 4.2. To evaluate the performance, all the classifiers are trained using the strategy described in Section 5.1. Thus, ten SVMs, ten fuzzy SVMs, and ten N-SVMs are generated, respectively. For each random split of the images, the same set of training data and test data is used in the corresponding SVM, fuzzy SVM, and N-SVM. Since the dataset is unbalanced, Eq. (4.23) is used to calculate the parameters of the weighting function g_j in N-SVM. The classification results are presented in Table 5.1.

Table 5.1: Average Classification Accuracy of the Proposed N-SVM, Standard SVM, and Fuzzy SVM on COREL 1000 Dataset, Respectively.

Classifier	Average Classification Accuracy
N-SVM	**87.7%**
SVM	82.2%
fuzzy SVM	84.3%

The results clearly show that the proposed N-SVM performs the best. It outperforms both the traditional SVM and fuzzy SVM in terms of the average classification accuracy by 5.5% and 3.4%, respectively. The weighting function of the N-SVM successfully reduces the effect of outliers and leads to a higher classification accuracy compared to the traditional SVM. As a generalization of a fuzzy set, a neutrosophic set introduces one more property "neutrality" to be associated with the inputs. Thus, the proposed N-SVM contains more information in the weighting function and achieves better results compared to the fuzzy SVM. In addition, the proposed system was also compared with the DD-SVM system in [46]. The classification accuracy of DD-SVM using the same dataset is 81.5%. N-SVM improves the accuracy by 6.2%.

Next, a closer analysis of the performance is made by looking at classification results on every category in terms of the confusion matrix. The classification results are listed in Table 5.2.

Table 5.2: Confusion Matrix of the Proposed N-SVM Using Eq. (4.23).

	Africa	Beach	Building	Bus	Dinosaur	Elephant	Flower	Horse	Mountain	Food
Africa	0.812	0.008	0.036	0.016	0.008	0.056	0.004	0.016	0.024	0.020
Beach	0.028	0.756	0.024	0.016	0.008	0.020	0.008	0.012	_0.120_	0.008
Building	0.036	0.040	0.836	0.008	0.004	0.016	0.012	0.008	0.016	0.024
Bus	0.004	0.008	0	0.980	0	0	0	0	0.004	0.004
Dinosaur	0	0	0	0	0.996	0	0	0	0	0.004
Elephant	0.024	0.004	0.008	0.004	0	0.880	0	0.012	0.036	0.032
Flower	0.008	0.004	0	0.008	0	0.004	0.936	0.008	0.008	0.024
Horse	0.008	0.008	0	0	0	0.008	0	0.964	0.004	0.008
Mountain	0.008	_0.148_	0.032	0.016	0.004	0.040	0.004	0.008	0.736	0.004
Food	0.032	0.016	0.008	0.012	0.008	0.020	0.012	0.008	0.008	0.876

Each row in Table 5.2 gives the average percentage of images in one category classified to each of the 10 categories by N-SVM using Eq. (4.23). The numbers on the diagonal (shaded) show the classification accuracy for each category, and off-diagonal entries indicate classification errors. According to the confusion matrix, the largest two errors (the underlined and italic numbers in Table 5.2) are the errors between the categories of "beach" and "mountains and glaciers." Twelve percent of the "beach" images are misclassified as "mountains and glaciers," while 14.8% of the "mountains and glaciers" images are misclassified as "beach." Figure 5.2 presents 10 misclassified images from both categories. All five "beach" images contain mountain-like regions, and all "mountains and glaciers" images contain regions corresponding to a lake or ocean. This may be the reason for the classification errors.

To further evaluate the performance of the proposed method, the same set of experiments was tested on Caltech 101 dataset. The results are given in Table 5.3.
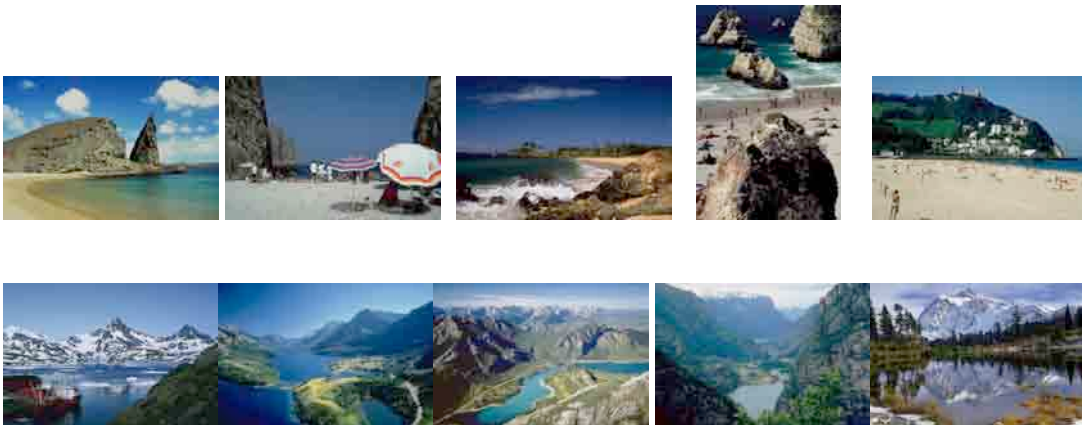

Fig. 5.2: Misclassified images from "beach" and "mountains and glaciers" categories.

Table 5.3: Average Classification Accuracy of the Proposed N-SVM, Standard SVM, and Fuzzy SVM on Caltech 101 Dataset, Respectively.

Classifier	Average Classification Accuracy
N-SVM	**65.9%**
SVM	61.6%
fuzzy SVM	63.5%

The results demonstrate that the proposed method still performs the best on a larger scale dataset. It outperforms both the traditional SVM and fuzzy SVM in terms of the average classification accuracy by 4.3% and 2.4%, respectively.

In summary, the experimental results demonstrate that the improvement of the classification accuracy is significant and adequately validates the correctness and effectiveness of the proposed reformulated SVM integrated with a neutrosophic set. Moreover, as a classification tool, the proposed N-SVM is independent of application. It can be applied to all classification problems wherein the traditional SVM is used, and theoretically it may achieve better results than the traditional SVM.

5.3 Evaluation of the Proposed Segmentation Method

To my knowledge, comparisons of the performance among different image segmentation algorithms are usually subjective. To evaluate the effectiveness of the proposed segmentation method, the categorization accuracy is adopted as the measurement. I compare the classification results of the proposed system with the ones

obtained from other segmentation approaches using the same classifiers. Here, the unsupervised *k*-means clustering algorithm is implemented for image segmentation as comparison. For fair comparison, all the following steps after segmentation are the same for both the k-means clustering and the proposed segmentation method. That is, for the regions obtained from each segmentation method, ten N-SVMs are trained respective to the weighting function calculated using Eq. (4.23). Table 5.4 gives the classification accuracy for the two methods tested on COREL 1000 dataset.

Table 5.4: Average Classification Accuracy of the Proposed Segmentation Algorithm and k-Means Clustering, Respectively.

Segmentation Method	Average Classification Accuracy
proposed algorithm	**87.7%**
k-means clustering	86.1%

The proposed segmentation method achieves a 1.6% improvement over the *k*-means clustering method in the average classification accuracy, which confirms the effect of the proposed segmentation algorithm when integrated into the image categorization problem. As concluded in [46], DD-SVM has low sensitivity to image segmentation. Thus, although the improvement of the accuracy is not that huge, it should demonstrate the effectiveness of the proposed segmentation method. The novel selection method in the proposed segmentation algorithm ensures that the training dataset contains more pixels representing the diverse regions in the image, rather than those representing the

homogeneous regions. Therefore, the training dataset obtained in this way carries more information than the training dataset generated by random selection, and it gives better results of segmentation. Furthermore, better segmentation results lead to better classification results in the region-based image categorization problem.

5.4 Analysis of the Effect of the Unbalanced Dataset

As discussed in Section 4.1, if the one-against-the-rest strategy is used to solve the multi-class problem, the training dataset for N-SVM will be unbalanced. The number of samples in the negative class is *m-1* times the number of samples in the positive class for *m* categories. To eliminate the unbalance, Eq. (4.23) is proposed as a modification to Eq. (4.20) when calculating the center of all the samples C_{all}. C_{all} calculated using Eq. (4.20) is the center simply based on the coordinates of the samples. Considering the unbalance property of the training dataset, the resulted C_{all} using Eq. (4.23) is the center of all the samples regarding to the data distribution in the input space.

In this section, I analyze the effects of the unbalanced dataset on the classification results. Two sets of 10 N-SVMs are designed using Eq. (4.20) and Eq. (4.23), respectively. They are trained using the same strategy as in Section 5.1. For each random split of the images, the same sets of training data and test data are used in the corresponding N-SVM of those two sets. Table 5.5 summarizes the classification results for the two sets of N-SVMs on COREL 1000 dataset.

Table 5.5: Classification Results of the Proposed N-SVM using Eq. (4.20) and Eq. (4.23), Respectively.

Classifier	Average Classification Accuracy
N-SVM using Eq. (23)	**87.7%**
N-SVM using Eq. (20)	86.7%

The results show that the N-SVM generated using the modified definition of C_{all} achieves a better classification accuracy compared with the N-SVM generated using Eq. (4.20). In Eq. (4.20), for the unbalanced dataset wherein the number of negative samples is multiple times of the number of positive samples, C_{all} is very close to the center of negative samples C_-. For a positive sample, its neutrosophic component i_j approaches f_j as observed from Eq. (4.21). As a result, the weighting function g_j of positive samples is almost only composed of t_j. Thus, the performance of the weighting function is weakened due to the unbalance of the training dataset. With the modified definition in Eq. (4.23), even for the unbalanced dataset, C_{all} is still in the middle of the center of positive samples C_+ and the center of negative samples C_-. The neutrosophic components associated with positive samples keep their attributes and contribute equally to weighting function g_j. Weighting function g_j acts as designed and reduces the effect of outliers. The experiment results also confirm this analysis. As discussed in Section 5.2, most of the misclassifications result from the semantic and visual similarity between the "beach" category and "mountains and glaciers" category, which is irrelevant to the unbalance

property of the dataset. Thus, although the improvement of the accuracy is 1%, it does validate that the modified definition of C_{all} helps eliminate the effects of unbalanced dataset.

CHAPTER 6

CONCLUSION

Neutrosophic logic is a relatively new logic that is a generalization of fuzzy logic. In this dissertation, for the first time, it is applied to the field of classifiers. The proposed classifier N-SVM is then evaluated under an image categorization system to validate its effectiveness. The main contributions are:

1. This dissertation is a brand new application of neutrosophic logic in pattern recognition. A novel reformulated SVM based on a neutrosophic set is proposed. Each input sample is associated with three neutrosophic components. A weighting function is designed based on the neutrosophic components to evaluate the degree of importance for each input in the training procedure. After integrating the proposed weighting function into the reformulated SVM, the achieved novel classifier N-SVM helps reduce the effects of outliers in the training samples. Experimental results show that the proposed classifier outperforms both the traditional SVM and fuzzy SVM in terms of classification accuracy under the discussed image categorization problem. Moreover, as a classification tool, the proposed N-SVM is independent of application. It can be applied to all the classification problems wherein the traditional SVM is used, and theoretically it may obtain better results than the traditional SVM.

2. An effective image segmentation method using a hierarchical SOM is adopted. To provide the optimal set of training samples for the HSOM, a novel approach to select training samples based on the homogeneity measure is proposed. The selection

approach ensures that the training dataset contains more pixels representing the diverse regions in the image, rather than those representing the homogeneous regions. The training dataset achieved in this way carries more information than the one obtained by random selection and leads to better segmentation results. The experimental results show that the proposed segmentation technique achieves higher classification accuracy in the categorization system than the unsupervised k-means clustering algorithm, which validates the effectiveness of the proposed segmentation method.

3. One-against-the-rest is a common technique to solve the multi-class problem encountered in most image categorization applications. As a result, the training dataset for N-SVM tends to be unbalanced. To eliminate the unbalance, a modified formula considering the sample distribution in the input space is proposed to calculate the center of all samples C_{all}. The experiment results validate that the modified definition of C_{all} helps eliminate the effects of an unbalanced dataset.

In summary, the application of neutrosophic logic to classifiers discussed in this dissertation has demonstrated good performance, as expected. By examining the experimental results, several aspects could be studied in the future. The future work for this dissertation is described as follows:

1. Neutrosophic logic could be applied to other kinds of classifiers such as neutral network, decision tree or the deep SVM in [47], etc. Moreover, it could also be applied to other research fields.

2. As discussed in Section 5.2, most of the classification errors in the experiment resulted from the semantic and visual similarity between the "beach" category and "mountains and glaciers" category. This phenomenon is very common in image categorization problems wherein class labels are associated with images. In fact, such keywords are often semantically related to respective regions rather than the entire image. Thus, in future work, one could associate keywords with regions in an image, and model the image categorization as a multi-label, multi-instance learning system to solve the problem and improve the classification accuracy.

REFERENCES

1. Smarandache, F.A. *A Unifying Field in Logics: Neutrosophic Logic. Neutrosophy, Neutrosophic Set, Neutrosophic Probability*. American Research Press, 2003.

2. Cheng, H.D. and Guo, Y. A new neutrosophic approach to image thresholding. *New Mathematics and Natural Computation 4*, 3 (2008), 291-308.

3. Zhang, M., Zhang, L., and Cheng, H.D. A neutrosophic approach to image segmentation based on watershed method. *Signal Processing 90*, 5 (2010), 1510-1517.

4. Juan, S., Cheng, H.D., and Wang, Y. A completely automatic segmentation method for breast ultrasound images using region growing. In *Proceedings of the 9th International Conference on Computer Vision, Pattern Recognition, and Image Processing*, 2008.

5. Guo, Y., Cheng, H.D., and Zhang, Y. A new neutrosophic approach to image denoising. *New Mathematics and Natural Computation 5*, 3 (2009), 653-662.

6. Yang, C., Dong, M., and Hua, J. Region-based image annotation using asymmetrical support vector machine-based multiple-instance learning. In *IEEE Computer Society Conference on Computer Vision and Pattern Recognition,* 2006, 2057-2063.

7. Abdullah, A., Veltkamp, R.C., and Wiering, M.A. Fixed partitioning and salient points with MPEG-7 cluster correlograms for image categorization**.** *Pattern Recognition 43*, 3 (2010), 650-662.

8. Sethi, I.K. and Coman, I.L. Mining association rules between low-level image features and high-level concepts. In *Proceedings of the SPIE Data Mining and Knowledge Discovery*, 2001, 279-290.

9. Chen, Y., Wang, J.Z., and Krovetz, R. An unsupervised learning approach to content-based image retrieval. In *IEEE Proceedings of the International Symposium on Signal Processing and its Applications*, 2003.

10. Smeulders, A.W.M., Worring, M., Gupta, A., and Jain, R. Content-based image retrieval at the end of the early years. *IEEE Trans. on Pattern Analysis and Machine Intelligence 22*, 12 (2000), 1349-1380.

11. Tao, D., Li, X., and Maybank, S. Negative samples analysis in relevance feedback. *IEEE Trans. on Knowledge and Data Engineering 19*, 4 (2007), 568-580.

12. Barnard, K., Duygulu, P., Forsyth, D., De Freitas, N., Blei, D.M., and Jordan, M.I. Matching words and pictures. *J. Machine Learning Research 3*, 3 (2003), 1107-1135.

13. Fan, J., Gao, Y., Luo, H., and Jain, R. Mining multilevel image semantics via hierarchical classification. *IEEE Trans. Multimedia 10*, 2 (2008), 167-187.

14. Duygulu, P., Barnard, K., de Freitas, J., and Forsyth, D.A. Object recognition as machine translation: Learning a lexicon for a fixed image vocabulary. In *Proceedings of the 7th European Conference on Computer Vision*, 2002.

15. Jeon, J., Lavrenko V., and Manmatha, R. Automatic image annotation and retrieval using cross-media relevance models. In *Proceedings of the 26th Annual International ACM SIGIR Conference on Research and Development in Information Retrieval*, 2003.

16. Lavrenko, V., Manmatha, R., and Jeon, J. A model for learning the semantics of pictures. In *Proceedings of 26th Advances in Neutral Information Processing*, 2003, 553-560.

17. Feng, S.L., Manmatha, R., and Lavrenko, V. Multiple bernoulli relevance models for image and video annotation. In *IEEE Computer Society Conference on Computer Vision and Pattern Recognition*, 2004.

18. Liu, J., Wang, B., Li, M., Li, Z., Ma, W., Lu, H., and Ma, S. Dual cross-media relevance model for image annotation. In *Proceedings of the 15th International Conference on Multimedia*, 2007.

19. Quelhas, P., Monay, F., Odobez, J.M., Gatica-Perez, D., Tuytelaars, T., and Gool, L.V. Modeling scenes with local descriptors and latent aspects. In *Proceedings of the 10th IEEE International Conference on Computer Vision*, 2005.

20. Blei, D.M. and Jordan, M.I. Modeling annotated data. In *Proceedings of the 26th Annual International ACM SIGIR Conference on Research and Development in Information Retrieval*, 2003.

21. Li, F. and Perona, P. A Bayesian hierarchical model for learning natural scene categories. In *Proceedings of the IEEE Conference on Computer Vision and Pattern Recognition*, 2005.

22. Lu, Z., Peng, Y., and Ip, H.H.S. Image categorization via robust pLSA. *Pattern Recognition Letters 31*, 1 (2010), 36-43.

23. Carneiro, G., Chan, A.B., Moreno, P.J., and Vasconcelos, N. Supervised learning of semantic classes for image annotation and retrieval. *IEEE Trans. Pattern Analysis and Machine Intelligence 29*, 3 (2007), 394-410.

24. Modestino, J.W. and Zhang, J. A Markov random field model-based approach to image interpretation. *IEEE Trans. Pattern Analysis and Machine Intelligence 14*, 6 (1992), 606-615.

25. Yu, H. and Wolf, W. Scenic classification methods for image and video database. In *Proceedings of the SPIE International Conference on Digital Image Storage and Archiving Systems*, 1995.

26. Li, J. and Wang, J.Z. Automatic linguistic indexing of pictures by a statistical modeling approach. *IEEE Trans. on Pattern Analysis and Machine Intelligence 25*, 9 (2003), 1075-1088.

27. Wang, L., Lu, Z., and Ip, H.H.S. Image categorization based on a hierarchical spatial Markov model. In *Proceedings of the 13th International Conference on Computer Analysis of Images and Patterns*, 2009.

28. Jin, R., Chai, J., and Si, L. Effective automatic image annotation via a coherent language model and active learning. In *Proceedings of the 12th Annual ACM International Conference on Multimedia*, 2004.

29. Jin, Y., Khan, L., and Wang, L. Image annotations by combining multiple evidence wordnet. In *Proceedings of the 13th Annual ACM International Conference on Multimedia*, 2005.

30. Kang, F., Jin, R., and Sukthankar, R. Correlated label propagation with application to multi-label learning. In *IEEE Conference on Computer Vision and Pattern Recognition*, 2006.

31. Feng, S. and Xu, D. Transductive multi-instance multi-label learning algorithm with application to automatic image annotation. *Expert Systems with Applications 37*, 1 (2010), 661-670.

32. Szummer, M. and Picard, R.W. Indoor-outdoor image classification. In *Proceedings of IEEE International Workshop on Content-Based Access of Image and Video Databases*, 1998.

33. Chapelle, O., Haffner, P., and Vapnik, V.N. Support vector machines for histogram-based image classification. *IEEE Trans. Neural Networks 10*, 5 (1999), 1055-1064.

34. Vailaya, A., Figueiredo, M.A.T., Jain, A.K., and Zhang, H.J. Image classification for content-based indexing. *IEEE Trans. Image Processing 10*, 1 (2001), 117-130.

35. Chang, E., Goh, K., Sychay, G., and Wu, G. CBSA: Content-based soft annotation for multimodal image retrieval using bayes point machines. *IEEE Trans. Circuits System and Video Technology 13*, 1 (2003), 26-38.

36. Huang, J., Kumar, S.R., and Zabih, R. An automatic hierarchical image classification scheme. In *Proceedings of the 6th ACM International Conference on Multimedia*, 1998.

37. Gdalyahu, Y. and Weinshall, D. Flexible syntactic matching of curves and its application to automatic hierarchical classification of silhouettes. *IEEE Trans. Pattern Analysis and Machine Intelligence 21*, 12 (1999), 1312-1328.

38. Gorkani, M.M. and Picard, R.W. Texture orientation for sorting photos 'at a glance.' In *Proceedings of the 12th International Conference on Pattern Recognition*, 1994.

39. Cusano, C., Ciocca, G., and Schettini, R. Image annotation using SVM. In *Proceedings of Internet Imaging SPIE 5304* (2004), 330-338.

40. Cheng, H.D., Datar, M., and Ju, W. Natural scene segmentation based on information fusion and homogeneity property. In *Proceedings of the 7th International Conference on Computer Vision, Pattern Recognition, and Image Processing*, 2006.

41. Cheng, H.D., Shan, J., Ju, W., Guo, Y., and Zhang, L. Automated breast cancer detection and classification using ultrasound images: A survey. *Pattern Recognition 43*, 1 (2010), 299-317.

42. Maron, O. and Lozano-Perez, T. A framework for multiple-instance learning. In *Proceedings of 11th Conference of Neural Information Processing Systems,* 1998, 570-576.

43. Qi, X. and Han, Y. Incorporating multiple SVMs for automatic image annotation. *Pattern Recognition 40*, 2 (2007), 728-741.

44. Li, R., Zhao, T., Zhang, Y., Xiao, Q., and Li, Y. Image annotation based on genetic feature selection and support vector machines. *Computer Engineering and Applications 45*, 6 (2009), 180-183.

45. Andrews, S., Tsochantaridis, I., and Hofmann, T. Support vector machines for multiple-instance learning. In *Advances in Neural Information Processing Systems 15*, Ed. MIT Press, 2003, 561-568.

46. Chen, Y. and Wang, J. Image categorization by learning and reasoning with regions. *J. Machine Learning Res. 5*, 12 (2004), 913-939.

47. Abdullah, A., Veltkamp, R.C., and Wiering, M.A. An ensemble of deep support vector machines for image categorization. In *International Conference of Soft Computing and Pattern Recognition*, 2009.

48. Cheng, H.D., Jiang, X.H., Sun, Y., and Wang, J.L. Color image segmentation: Advances and prospects. *Pattern Recognition 34*, 12 (2001), 2259-2281.

49. Kohonen, T. The self-organizing map. *Proceedings of the IEEE 78*, 9 (1990), 1464-1480.

50. Lampinen, J. and Oja, E. Clustering properties of hierarchical self-organizing maps. *J. Mathematical Imaging and Vision 2*, 2-3 (1992), 261-272.

51. Laws, K.I. Texture energy measures. In *Proceedings of Image Understanding Workshop*, 1979, 47-51.

52. Laws, K.I. *Textured Image Segmentation*. PhD Thesis, University of Southern California, 1980.

53. Cheng, H.D. and Sun, Y. A hierarchical approach to color image segmentation using homogeneity. *IEEE Trans. Image Processing 9*, 12 (2000), 2071-2082.

54. Cheng, H.D., Xue, M., and Shi, X. Contrast enhancement based on a novel homogeneity measurement. *Pattern Recognition 36*, 11 (2003), 2687-2697.

55. Vapnik, V. *The Nature of Statistical Learning Theory*. Springer, 1995.

56. Lin, C.F. and Wang, S.D. Fuzzy support vector machines. *IEEE Trans. Neural Networks 13*, 2 (2002), 464-471.

57. Ju, W., Shan, J., Yan, Y., and Cheng, H.D. Discrimination of outer membrane proteins using fuzzy support vector machines. In *Proceedings of the 8ᵗʰ International Conference on Computer Vision, Pattern Recognition, and Image Processing*, 2007.

58. Wang, J.Z., Li, J. and Wiederhold, G. SIMPLIcity: Semantics-sensitive integrated matching for picture libraries. *IEEE Trans. Pattern Analysis and Machine Intelligence 23*, 9 (2001), 947-963.

59. Min, R. and Cheng, H.D. Effective image retrieval using dominant color descriptor and fuzzy support vector machine. *Pattern Recognition 42*, 1 (2009), 147-157.

60. Wang, T. and Chiang, H. Fuzzy support vector machine for multi-class text categorization. *Information Processing and Management 43*, 4 (2007), 914-929.

CURRICULUM VITAE

Wen Ju

Email: wen.ju@aggiemail.usu.edu Phone: (408) 916-8981

Summary

- 6+ years' experience in C/C++, C#, Matlab;
- Strong background in mathematics, data structure and algorithms.
- 5+ years' experience in research and development in image processing, pattern recognition, computer vision, and fuzzy logic;
- Strong experience in machine learning techniques including Neural Network, Self Organizing Map, Support Vector Machine;
- In-depth knowledge of Java, ASP.net, SQL, MPI (parallelism) and R (a statistical tool);
- Rich experiences in Windows, Mac OS and Linux;

Education

Ph.D. in Computer Science
Utah State University, Logan, UT   August 2002 – May 2011 (expected)
Dissertation Topic: Novel application of neutrosophic logic in classifiers evaluated under
                region-based image categorization system
GPA: 3.92/4.0

Special Class for the Gifted Young
Bachelor of Computer Science
University of Science & Technology of China, Anhui, China September 1997-June 2002

Professional Experience

Research Work:

- *Color Image Processing*:
  - ➢ Color image segmentation based on homogeneity property using self organizing map;
  - ➢ Face detection in color images using fuzzy logic based on skin color distribution and contour map of eye-mouth triangle;

- *Pattern recognition*:
  - ➢ Developed a reformulated support vector machine (SVM) with multi-scale kernel, which improved the classification accuracy several bioinformatics applications.
  - ➢ Developed a reformulated SVM using neutrosophic set, which improved the performance of region-based image categorization.
- *Medical Image Processing*:
  - ➢ The preprocessing (speckle removal and image enhancement) of ultrasound images for automated breast cancer diagnosis;
  - ➢ Detection and classification of masses for breast cancer using fuzzy support vector machine;

Class Projects:

- Designed a wireless localization model to help robot locate its position;
- Designed a tool with SQL database to schedule the workload of multiple product lines, and achieve the maximum overall capacity.
- Designed an artificial brain to solve the "Knight's Tour" puzzle;
- Developed a classification tool based on Gene Expression Programming (GEP), which is a brunch of Neural Network;
- Designed a data mining model to evaluate business websites by crawling the internet, parsing web sources, and analyzing the extracted keywords;

Honors & Activities

- Teaching assistances including lab lecturing and grading homework, term projects and exams, Utah State University, 2004-2009
- Vice President Fellowship, Utah State University, 2002-2004
- Certification of excellent performance in the undergraduate research program "the quantification and parallel computation of the brain wave", 2001
- Scholarships, Special Class for the Gifted Young, University of Science & Technology of China, 1997-2000

Publications

Journal Papers:

- **Wen Ju**, Juan Shan, Changhui Yan and H.D. Cheng, "Discrimination of Disease-Related non-Synonymous Single Nucleotide Polymorphism using Multi-Scale RBF Kernel Fuzzy Support Vector Machines", *Pattern Recognition Letters,* pp.391-396, vol. 30, 2009.

- H.D. Cheng, Juan Shan, **Wen Ju,** Yanhui Guo and Ling Zhang, "Automated Breast Cancer Detection and Classification using Ultrasound Images: A Survey", *Pattern Recognition,* pp. 299-317, vol. 43, 2010.
- Xiangjun Shi, H.D. Cheng, Liming Hu, **Wen Ju** and Jiawei Tian, "Detection and Classification of Masses in Breast Ultrasound Images", *Digital Signal Processing*, pp. 824-836, vol. 20, 2010.

Conference Papers:

- **Wen Ju** and H.D. Cheng, " Discrimination of Outer Membrane Proteins using Reformulated Support Vector Machine based on Neutrosophic Set", *Proc. of the 9th International Conference on Computer Vision, Pattern Recognition, and Image Processing (CVPRIP'08)*, 2008.
- Juan Shan, **Wen Ju**, Changhui Yan and H. D. Cheng, "Discrimination of Disease-Related Non-Synonymous Single Nucleotide Polymorphism using Fuzzy Support Vector Machine", *Proc. of the 8th International Conference on Computer Vision, Pattern Recognition, and Image Processing (CVPRIP'07)*, pp. 861-867, 2007.
- **Wen Ju**, Juan Shan, Changhui Yan and H.D. Cheng, "Discrimination of Outer Membrane Proteins using Fuzzy Support Vector Machines", *CVPRIP'07*, pp. 854-860, 2007.
- Heng-Da Cheng, Manasi Datar and **Wen Ju**, "Natural Scene Segmentation based on Information Fusion and Homogeneity Property", *Proc. of the 7th International Conference on Computer Vision, Pattern Recognition, and Image Processing (CVPRIP'06)*, 2006.